Pharmaceutical Research, Vol. 25, No. 7, July 2008 (© 2008)
DOI: 10.1007/s11095-008-9561-z

Research Paper

Intra and Inter-Molecular Interactions Dictate the Aggregation State of Irinotecan Co-Encapsulated with Floxuridine Inside Liposomes

Awa Dicko,[1] April A. Frazier,[1] Barry D. Liboiron,[1] Anne Hinderliter,[2] Jeff F. Ellena,[3] Xiaowei Xie,[1] Connie Cho,[1] Tom Weber,[1] Paul G. Tardi,[1] Donna Cabral-Lilly,[4] David S. Cafiso,[3] and Lawrence D. Mayer[1,5]

Received December 14, 2007; accepted February 19, 2008; published online March 5, 2008

Purpose. The inter/intramolecular interactions between drugs (floxuridine, irinotecan) and excipients (copper gluconate, triethanolamine) in the dual-drug liposomal formulation CPX-1 were elucidated in order to identify the physicochemical properties that allow coordinated release of irinotecan and floxuridine and maintenance of the two agents at a fixed, synergistic 1:1 molar ratio.
Methods. Release of irinotecan and floxuridine from the liposomes was assessed using an *in vitro*-release assay. Fluorescence, Nuclear Magnetic Resonance spectroscopy (NMR) and UV–Vis were used to characterize the aggregation state of the drugs within the liposomes.
Results. Coordinated release of the drugs from liposomes was disrupted by removing copper gluconate. Approximately 45% of the total irinotecan was detectable in the copper-containing CPX-1 formulation by NMR, which decreased to 19% without copper present in the liposomal interior. Formation of higher order, NMR-silent aggregates was associated with slower and uncoordinated irinotecan release relative to floxuridine and loss of the synergistic drug/drug ratio. Solution spectroscopy and calorimetry revealed that while all formulation components were required to achieve the highest solubility of irinotecan, direct drug-excipient binding interactions were absent.
Conclusions. Long-range interactions between irinotecan, floxuridine and excipients modulate the aggregation state of irinotecan, allowing for simultaneous release of both drugs from the liposomes.

KEY WORDS: copper gluconate; CPX-1; rotational diffusion; spectroscopy; triethanolamine.

INTRODUCTION

The use of nanoscale carriers has expanded beyond applications with single therapeutic agents to systems designed for delivery of drug combinations in a coordinated fashion. Examples include nanoscale delivery systems that first expose solid tumors to an anti-angiogenesis agent to cause vascular collapse followed by the slow release of a cytotoxic agent to kill the tumor cells directly (1), as well as combinations co-formulated to maintain fixed drug ratios after administration *in vivo* (2). The latter approach relates to recent evidence that the therapeutic activity of many anticancer drug combinations is dependent on the molecular ratio of the combined drugs, where certain ratios can interact synergistically while other ratios of the same agents can be antagonistic (2,3). Liposomal carriers have been applied to combination therapy to develop formulations that efficiently co-encapsulate two antineoplastic agents in a single liposome and maintain their ratio in the plasma after i.v. administration, overcoming disparate *in vivo* clearance mechanisms that typically disrupt the ratio of injected drugs when administered as a free drug cocktail. A similar concept was more recently used to co-encapsulate fludarabine and mitoxantrone in liposomes for the potential treatment of leukemia and lymphoma (4).

CPX-1 is a liposomal formulation of irinotecan and floxuridine that maintains the synergistic 1:1 molar ratio of the two drugs for up to 24 h in the plasma of mice and humans while at the same time makes the drugs bioavailable (2,3,5–9). CPX-1 has demonstrated dramatically increased therapeutic activity in preclinical tumor models compared to free drug cocktail and has provided encouraging signs of therapeutic activity in clinical trials (6,7). The importance of maintaining the 1:1 molar ratio of irinotecan/floxuridine is highlighted in Table I. Liposome formulations were prepared containing irinotecan/floxuridine molar ratios of 10:1, 1:1 and 0.1:1. Previous studies (2) demonstrated that *in vitro*, the 10:1 drug ratio is antagonistic in the HT-29 human colorectal cancer cell line and the 0.1:1 drug ratio is antagonistic in the Capan-1 human pancreatic cancer cell line. In both tumor

Electronic supplementary material The online version of this article (doi:10.1007/s11095-008-9561-z) contains supplementary material, which is available to authorized users.

[1] Celator Pharmaceuticals Corp., 1779 W 75th Avenue, Vancouver, British Columbia V6P 6P2, Canada.
[2] Department of Chemistry and Biochemistry, College of Science and Engineering, University of Minnesota-Duluth, 1039 University Drive, Duluth, Minesota 55812-3020, USA.
[3] Department of Chemistry, University of Virginia, McCormick Road, P.O. Box 400319, Charlottesville, Virginia 22904-4319, USA.
[4] Celator Pharmaceuticals Inc., 303B College Road East, Princeton, New Jersey 08540, USA.
[5] To whom correspondence should be addressed. (e-mail: lmayer@celatorpharma.com)

Table I. Drug Ratio Dependent *In Vivo* Efficacy of Irinotecan/Floxuridine Combinations Co-Encapsulated Inside 100 nm DSPC/DSPG/Chol (7:2:1) Liposomes

Irinotecan/Floxuridine Molar Ratio Inside Liposomes	Plasma Irinotecan/Floxurdine Molar Ratio Range over 24 h[a]	Log Cell Kill at MTD[b]	
		HT-29	Capan-1
10:1	7.2–15.3	1.48	ND
1:1	0.93–1.43	1.71	1.81
0.1:1	0.07–0.13	ND	0.56

Adapted from (2)
MTD maximum tolerable dose, *ND* not determined
[a] Drug levels determined by HPLC in plasma samples collected from mice after intravenous injection of CPX-1 [2]
[b] Log cell kill = $[T - C]/(3.32 \times T_d)$ where $T - C$ is the treatment induced delay for tumors to reach a specified size and T_d is the tumor doubling time (7 days for both tumor models)

lines, the 1:1 molar ratio was strongly synergistic. When these liposome formulations were administered intravenously to mice, the plasma irinotecan/floxuridine ratio was maintained very near the formulated drug ratio over 24 h (Table I). This allowed us to test whether the efficacy of this drug combination was drug ratio dependent *in vivo*. The degree of antitumor activity can be quantified by determining the log cell kill (LCK) provided by treatments based on the delay in tumor growth to a pre-specified size (2). In the HT-29 solid tumor model, the synergistic 1:1 molar ratio was more efficacious than the 10:1 molar ratio and in fact, the 10:1 molar ratio was less efficacious than liposomal irinotecan alone. Similarly, the synergistic 1:1 molar ratio was markedly more efficacious than the antagonistic 0.1:1 molar ratio in the Capan-1 solid tumor model and the antagonist combination was approximately fivefold less active than liposomal irinotecan alone. Consequently, it is clear that optimal therapeutic activity *in vivo* is dependent on maintaining the molar ratio of irinotecan/floxuridine near 1:1 as significant divergence in either direction could lead to loss of efficacy.

The importance of characterizing co-formulated drug combination delivery systems stems from the fact that the physicochemical interactions between drugs and excipients likely modulate the drug disposition and physical state inside liposomes which ultimately will dictate drug release and *in vivo* performance. We have demonstrated that liposomes containing copper gluconate/triethanolamine (TEA) at pH 7.0 are able to actively sequester irinotecan (5) without employing acidic pH gradients that could lead to lipid and/or drug instability during storage due to acid-mediated hydrolysis (10–14). Although unbuffered copper sulfate can be used to encapsulate irinotecan, high copper concentrations are required and the pH inside the liposomes is very low (pH 3.5). To reduce the amount of copper required and maintain the pH near neutrality, copper gluconate was chosen and was found to be superior in percentage encapsulation and drug retention compared to copper sulfate (5). Subsequent investigations revealed that the loading of irinotecan into liposomes was mediated by a charge-neutral stoichiometric exchange of TEA out of the liposome with concurrent irinotecan exchange into the liposome resulting in irinotecan self-association upon accumulation (15).

We have previously shown that coordinated release of irinotecan and floxuridine could be achieved by altering the concentration of cholesterol (Chol) of distearoylphosphatidylcholine/ distearoylphosphatidylglycerol (DSPC/DSPG) based formulations containing copper gluconate/TEA (5). The retention of floxuridine in plasma was optimal in formulations with less than 20 mol% cholesterol while increasing cholesterol concentration enhanced irinotecan retention. CPX-1 liposomes composed of DSPC/DSPG/Chol, 7:2:1 exhibited matched release rates for both drugs that were maintained for prolonged time after *in vivo* administration (5). Additional characterization of CPX-1 revealed that the release of irinotecan could also be dependent on its aggregation state inside liposomes (15). Floxuridine and numerous excipients present inside CPX-1 liposomes may interact with irinotecan, individually or in combination, and this could dictate the self-association of irinotecan. Therefore, in the present study, an in-depth characterization of the interactions of irinotecan with floxuridine, copper gluconate and TEA was undertaken in order to establish the physicochemical features that control irinotecan release from liposomes.

MATERIAL AND METHODS

Materials

Distearoylphosphatidylglycerol (DSPG) and distearoylphosphatidylcholine (DSPC) were purchased from Lipoid (Newark, NJ, USA). Cholesterol (Chol) was obtained from Solvay (Houston, TX, USA). Irinotecan hydrochloride trihydrate was obtained as a dry powder from ScinoPharm Taiwan, Ltd. (Tainan, Taiwan). Floxuridine was obtained from the Zhejiang Hisun Pharmaceutical Company (Taizhou City, China). Copper gluconate was purchased from Purac (Lincolnshire, IL, USA). All other chemicals were obtained from Sigma Chemical Company (St. Louis, MO, USA).

Preparation of the Formulations

The formulations were prepared by a process where irinotecan and floxuridine are encapsulated in pre-formed liposomes generated by a solvent emulsion and size reduction procedure as previously described (5,15). Briefly, the lipids (DSPC/DSPG/Chol, 7:2:1, mol%) were dispersed in solutions of 100 mM copper gluconate/180 mM TEA (pH 7.0, referred to as CPX-1) or 10 mM sodium gluconate/180 mM TEA (pH 7.0, referred to as copper-free formulation). The liposomes were extruded at 70°C through two stacked 100 nm polycarbonate filters using a water jacketed extrusion apparatus. The external buffer was exchanged for sucrose phosphate EDTA buffer at pH 7.0 (SPE) using tangential flow chromatography. The coencapsulation of irinotecan and floxuridine was carried out by mixing the drug solution and the liposomes for 1 h at 50°C. The unencapsulated drugs were removed by exchanging the external liposomal buffer into sucrose phosphate buffer at pH 7.0 (SP) using tangential flow chromatography.

In Vitro Release (IVR) Assay

CPX-1 or the copper-free formulations were added to the phosphate incubation buffer (Octyl β-D-glucopyranoside

(OGP)/EDTA, pH 5.25) preheated at 37°C in a shaking water bath. Aliquots collected at selected timepoints over 24 h were centrifuged at 10,000×*g* for 20 min using Microcon YM-100 centrifugal filters units (Millipore, Billerica, MA) to separate the encapsulated material from the released drugs. Irinotecan and floxuridine were assayed by high performance liquid chromatography (HPLC) using Waters C_{18} reverse phase columns. The percentage of drug release was calculated as the molar ratio of free drug to total drug.

Cryogenic Transmission Electron Microscopy

The cryogenic transmission electron microscopy (cryo-EM) investigations were performed with a Zeiss EM 902A Transmission Electron Microscope (Carl Zeiss NTS, Oberkochen, Germany). The procedure used for sample preparation and image recording is described in Almgren *et al.* (16). Briefly, a small drop (~1 μl) of sample was deposited on a copper grid covered with a perforated polymer film covered with a thin carbon layer on both sides. Excess liquid was removed by means of blotting with a filter paper, leaving a thin film of the solution on the grid. Immediately after blotting, the sample was vitrified in liquid ethane, held just above its freezing point. Samples were kept below −165°C and protected against atmospheric conditions during both transfer to the microscope and examination. Images were recorded under low dose conditions at 105,000× magnification with a defocus of 3 μm.

Nuclear Magnetic Resonance (NMR) Spectroscopy

Sample Preparation

The peaks of the external SP buffer solution of CPX-1 interfere with those of the internal liposomal components. To resolve this problem, the external SP buffer was replaced with an approximate iso-osmotic buffer of 150 mM sodium chloride (NaCl) or 150 mM NaCl/40 mM sodium phosphate, pH 7.0 in deuterium oxide (D_2O). Four aliquots of 75 μl of liposomes were applied to a Sephadex G-50, 1 ml spin column. The liposome fraction was collected in the void volume by centrifuging at 515×*g* for 2 min. The samples were diluted to 3 mM irinotecan and/or 3 mM floxuridine. 3-(trimethylsilyl)-1-propansulfonic acid (DSS; Sigma-Aldrich Canada, Oakville, ON) was used as an internal chemical shift and intensity standard.

^{1}H NMR Measurements

One dimensional proton NMR (1D ^{1}H NMR) spectra were acquired on a Bruker Avance 400 MHz spectrometer (Bruker Biospin, Milton, ON). Advanced Chemistry Development's (ACD) 1D/2D NMR Processor was used to analyze the NMR data (Advanced Chemistry Development, v. 10.01, Toronto, ON). Linewidth measurements were made as the full width at half maximum (FWHM) of calculated Lorentzian-Gaussian (1:1) peaks, iteratively fitted to the experimental spectrum through a least squares routine in the ACD software.

Integration of irinotecan and floxuridine proton resonant peak intensities (in the region 6–8 ppm) was used as a means to determine the concentration of the freely soluble portion of each drug in the liposomal formulations, using the common assumption that precipitated and/or highly aggregated drug portions (if present) are NMR-silent. Resonant peak full width at half maximum (FWHM) was used as an indicator of the tumbling rate (and hence size) of the molecule under study, using the well-characterized globular protein ubiquitin amide as a linewidth standard of known molecular morphology (i.e. spherical) and weight (8.6 kDa). A full description of the relationships between molecule size, tumbling rate and NMR linewidth is given in the Discussion section.

Ultraviolet–Visible (UV–Vis) Spectroscopy

Samples of increasing concentrations of irinotecan were made by dissolving the drug powder in water at 50°C. UV–Vis spectroscopy was carried out on a Shimadzu UV-2401PC (Shimadzu Scientific Instruments, Columbia, MD) and a Varian Cary 4000 equipped with a 6×6 Peltier sample holder (Varian, Palo Alto, CA). A wavelength range of 280–500 nm was collected and a slit width of 1.0 nm was used. Measurements were made at ambient temperature using quartz cells with a 10 or 1 mm path length.

Fluorescence Spectroscopy

Samples were prepared with increasing concentrations of irinotecan in water to approximately 1 mM. Duplicates of these titration samples were prepared in the presence of 1 mM floxuridine or 1 mM copper gluconate/TEA. The measurements were made using a Varian Cary Eclipse fluorescence spectrophotometer (Varian, Palo Alto, CA). Data were collected at room temperature using a small cuvette. The excitation wavelength was 425 nm.

Isothermal Titration Calorimetry

Isothermal titration calorimetry (ITC) experiments were carried out on a Microcal VP-ITC (Microcal, Northampton, MA). Each experiment was carried out at 25°C in high feedback mode/gain, and a reference power of 10 μCal/s. The spacing between each injection varied between experiments over a range of 300 to 480 s required to reestablish a stable baseline. Data analysis was carried out using Origin 7.0 (Originlab, Northampton, MA).

Irinotecan Solubility Assay

Irinotecan absorbs light readily and has an extinction coefficient at 370 nm of 22,500±200 M^{-1} cm^{-1} whether in double distilled water or SP buffer. Irinotecan was added to the following solutions at a theoretical concentration of 85 mM:

1. Water
2. 90 mM floxuridine
3. 100 mM copper gluconate/180 mM TEA, pH 7.0
4. 100 mM copper gluconate/180 mM TEA, pH 7.0+ 90 mM floxuridine
5. 10 mM sodium gluconate/180 mM TEA, pH 7.0

Samples were heated at 50°C, vortexed, pH adjusted to 7.0 using NaCl or HCl, then centrifuged at 2,500×*g* for 10 min

to pellet any undissolved irinotecan. One milliliter aliquots from the supernatant were taken and placed in 1.5 ml Eppendorf tubes. These tubes were spun for an additional 10 min at 15,000×*g* to pellet any remaining undissolved irinotecan. By visual inspection, the solutions were clear when samples were taken for absorbance measurements. UV–Vis absorbance readings were taken on a Shimadzu UV-2401PC (Shimadzu Scientific Instruments, Columbia, MD). Due to the concentrated nature of the solutions, the aliquots were diluted to an appropriate concentration with water, such that the absorbance reading was below 1.5.

RESULTS

Effect of Entrapped Copper Gluconate on the Physical State of Irinotecan and Floxuridine Inside Liposomes

In a previous study, we demonstrated that TEA mediated irinotecan encapsulation into copper gluconate/TEA containing liposomes (15). We speculated that irinotecan interacted with neighboring drug molecules resulting in larger supramolecular complexes that were retained inside the liposomes. To elucidate the impact of copper gluconate on the drug's aggregation state, we designed a copper-free formulation containing the same amount of TEA as in CPX-1 that was capable of encapsulating both irinotecan and floxuridine in a similar TEA-dependent manner. The internal buffer of the copper-free formulation consisted of 10 mM sodium gluconate/180 mM TEA, pH 7.0.

An *in vitro* drug release (IVR) assay was performed to compare the release rate of irinotecan from copper-free and CPX-1 liposomes. The performance of CPX-1 relies on maintaining the 1:1 ratio for both floxuridine and irinotecan and avoiding significant deviation from this synergistic ratio is critical for optimal therapeutic activity. The IVR assay was designed as a simple, reproducible, sensitive and validateable tool to detect changes in drug release from different formulations that may affect performance. It also provides a valuable quality control measure to assure batch-to-batch uniformity. In this assay, the liposomes were incubated at 37°C in the presence of a membrane perturbing surfactant (OGP) that induced increased membrane permeability to mimic conditions *in vivo*. Drug released from the liposomes was determined by quantifying the concentration of drug in the filtrate after ultrafiltration of the test solution whereas the liposomes and entrapped contents were retained in the retentate reservoir. Figure 1 shows similar floxuridine release rates from both CPX-1 and copper-free liposomes when incubated over 24 h at 37°C. Approximately 50% of the entrapped irinotecan was released from CPX-1 within 6 h at 37°C, but irinotecan release from copper-free liposomes was only 25% at 6 h and less than 45% after 24 h at 37°C, compared to greater than 60% for CPX-1.

Interestingly, cryo-EM analysis of CPX-1 did not reveal any morphological features that were distinct from the copper-free formulation. As shown in Fig. 2, there was no evidence of drug crystallization or precipitation inside the liposomes and also no apparent changes in the membrane structure were observed. Both liposomes presented a regular, faceted polyhedral surface morphology. Occasionally, an additional internal lamellae or an electron dense line was observed in the liposomes interior. This feature was attributed to invaginated planes of gel phase lipid arising from the polyhedral shape of the liposomes since such structures were also present in the liposomes prior to drug loading (data not shown).

To delineate the physicochemical basis for the differences in irinotecan IVR results for CPX-1 and copper-free liposomes, proton NMR spectra were acquired on both formulations and the free drugs in solution. The solution state NMR spectrum in the aromatic region of an equimolar mixture of irinotecan and floxuridine is shown in Fig. 3a. Peaks in the aromatic region were assigned to either floxuridine or irinotecan through measurement of the individual drugs in solution (data not shown). The aromatic protons of irinotecan appear at approximately 7.2, 7.7 and 7.8 ppm while floxuridine has two doublets centered at 7.4 and 8.0 ppm. Figure 3b shows the ^{1}H NMR spectrum of CPX-1 (1) and the copper-free formulation (2) in the 5–9 ppm region. Peak identities were assigned using individual liposomal drugs spectra (data not shown) and were shifted compared to the solution state spectrum. Casual inspection

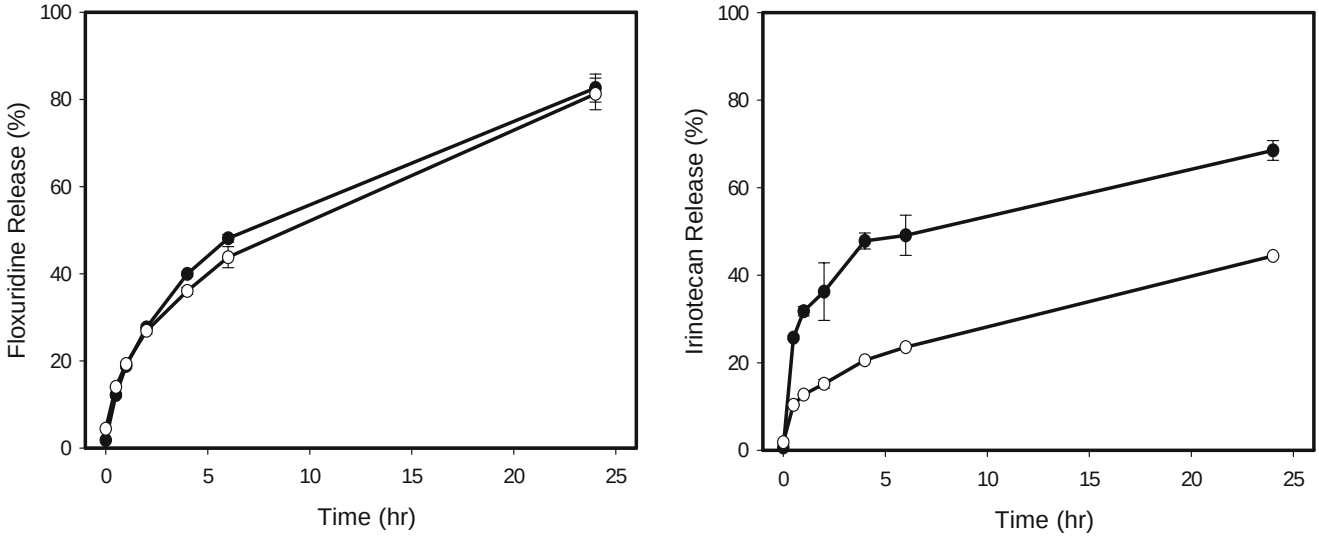

Fig. 1. *In vitro* release of floxuridine and irinotecan from CPX-1 (*filled circle*) and copper-free liposomes (*open circle*).

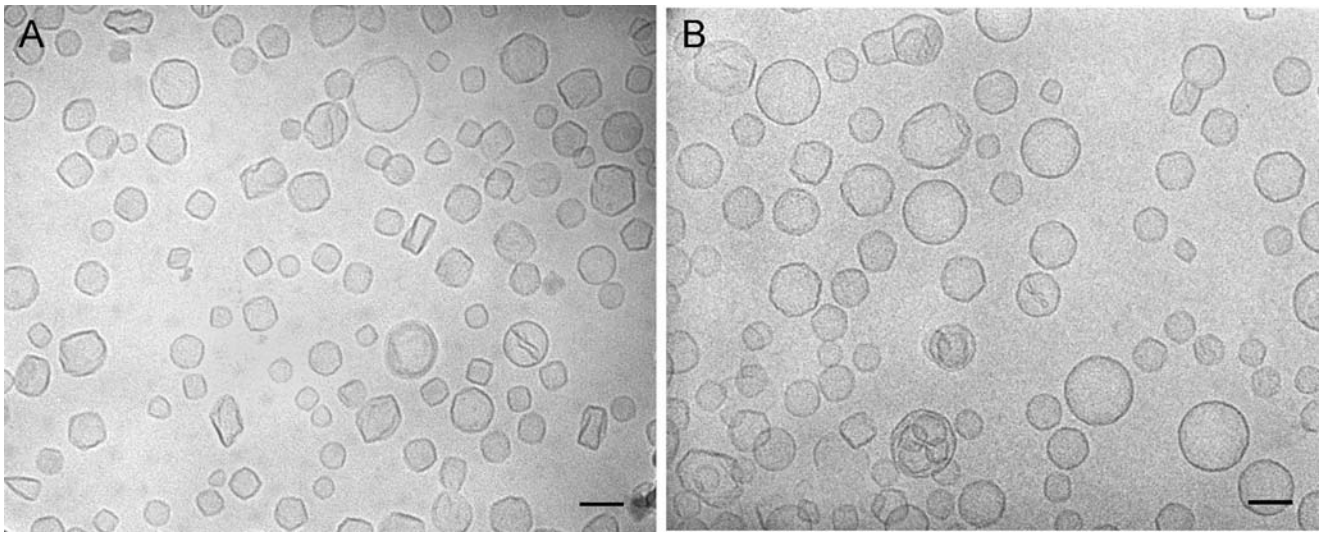

Fig. 2. Cryo-electron micrographs of (**A**) CPX-1 and (**B**) copper-free formulations. The scale bar represents 100 nm.

reveals a clear broadening of the aromatic proton signals (between 6 and 8 ppm) for both formulations relative to the free drugs and a reduction in irinotecan peak intensities relative to the floxuridine peaks. Additionally, irinotecan peak intensities are smaller in the copper-free formulation relative to CPX-1.

The integrated intensities of floxuridine and irinotecan downfield peaks between 6 and 8 ppm in the copper-free and CPX-1 formulations are presented in Table II. The intensity of the DSS peak at 0 ppm was used as an internal concentration standard such that its integral was set to a value equal to the DSS concentration in millimolar units. Thus, floxuridine concentration can be gauged directly from the integrated intensity reported in Table II as the high field (HF, at ~6.1 ppm) and low field (LF, at ~7.8 ppm) peaks each correspond to one proton. A large proportion of the available floxuridine (3 mM) is observed by ^{1}H NMR in both samples; 94% of the drug is accounted for in the copper-free formulation while approximately 75% of the total floxuridine is detected in CPX-1. The increased line broadening of floxuridine peaks in CPX-1 is likely due to paramagnetic broadening from the copper gluconate/TEA buffer system.

For irinotecan, the peaks between 6.5 and 7.5 ppm (Fig. 3b) correspond to four aromatic protons. If 100% of the irinotecan were observed, an integrated intensity of 12 (4×3 mM) would be measured. The data in Table II show that in the case of the copper-free formulation, only approximately 19% of the available irinotecan can be observed in the ^{1}H NMR spectrum. For CPX-1, this value increases to approximately 45%.

In both formulations, the NMR peaks of the two drugs are very broad compared to the spectrum in solution (Table III). Irinotecan line broadening is similar in the copper-free *versus* the CPX-1 formulation: linewidths at 7.25 ppm are 56 and 52 Hz, respectively, compared to 2–3 Hz for the comparable signals in a solution of free irinotecan. At 7.1 ppm, the

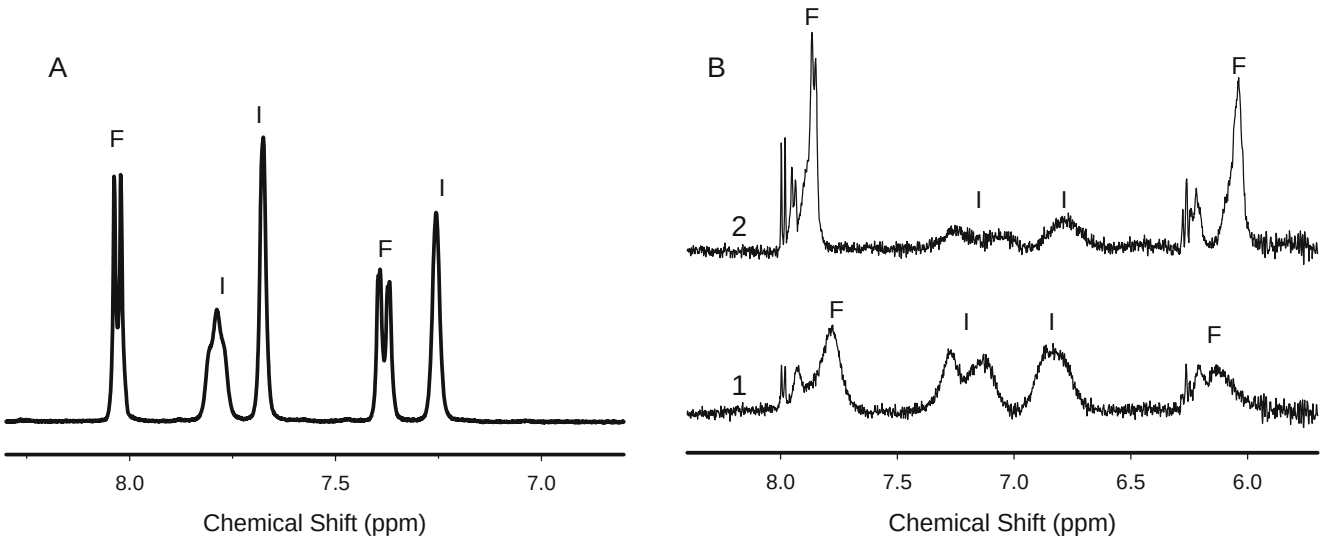

Fig. 3. Proton NMR spectra of (**A**) a mixture of 3 mM irinotecan (*I*) and 3 mM floxuridine (*F*) in water; (**B**) CPX-1 (*1*) and copper-free liposomes (*2*).

Table II. Integrated NMR Signal Intensities of Floxuridine and Irinotecan Relative to the Internal DSS Concentration Standard for the Copper-Free and CPX-1 Formulations (Drug Concentrations are 3 mM)

Sample	Low Field Floxuridine	Irinotecan	High Field Floxuridine	% Floxuridine Observed[b]	% Irinotecan Observed[b]
Protons	1	4	1	–	–
Copper-free	2.82	2.24	2.94	94.0	18.7
CPX-1	2.50	5.39	1.71[a]	75.0	44.9

[a] The integrated intensity of this peak is reduced due to the presence of paramagnetic Cu(II) in the copper gluconate buffer. Analysis of T_1 relaxation times (data not shown) indicate that only this peak is susceptible to augmented relaxation and decreased intensity due to transient Cu(II) coordination to a small portion of the available floxuridine. This feature has the effect of reducing the observable floxuridine for this peak only. The low field peak of the CPX-1 sample was used to determine the amount of observable floxuridine.
[b] Calculated as the integrated intensity divided by the number of protons, multiplied by the DSS concentration to yield the concentration of observable drug.

linewidth is less for CPX-1 (29 Hz) *versus* the copper-free formulation (49 Hz). The peaks of floxuridine appear sharper in the copper-free sample compared to CPX-1, suggesting that this broadening effect is due to the presence of paramagnetic copper ions. The full width at half maximum (FWHM) of two of the aromatic proton resonances for irinotecan in solution and the two liposomal formulations are reported in Table III. For comparison, the reported linewidth of the protons of ubiquitin amide (6 Hz), a 8.6 kDa globular protein, is also listed (17). At constant temperature, the resonant linewidth is directly proportional to the spin-spin (T_2) relaxation time in NMR, which in turn is a product of the rotational correlation time of the molecule under study. Slow molecular tumbling leads to augmented T_2 (transverse) spin-spin relaxation rates that can measurably broaden the resonant proton signals, and in extreme cases, thwart detection of the proton in the NMR experiment (18). As the molecular dynamics of ubiquitin amide are well studied, it is useful for comparison as a large macromolecule of roughly spherical shape against the tumbling behavior of NMR-detectable irinotecan aggregates in CPX-1.

Solution State Characterization of Irinotecan

The above NMR data indicated that the state of irinotecan aggregation in CPX-1 was different from that in the copper-free formulation and this, in turn, correlated with altered irinotecan *in vitro* release kinetics. Thus, a systematic characterization study was undertaken to identify the nature of interactions between excipients and drugs in CPX-1 that could impact the self-association state of irinotecan. This study was performed in solution to avoid interferences from the liposomes.

Table III. Full Width at Half Maximum (FWHM, in Hertz) of Irinotecan Proton NMR Resonances for Irinotecan in Solution and in the CPX-1 and Copper-Free Liposomal Formulations (Drug Concentrations are 3 mM)

	Peak 1		Peak 2	
Sample	FWHM	δ (ppm)	FWHM	δ (ppm)
Solution	3.4	7.75	2.1	7.350
CPX-1	56	7.25	29	7.12
Copper-free	52	7.25	49	7.06
Ubiquitin amide	6 Hz			

Influence of Floxuridine and CPX-1 Excipients on Irinotecan Solubility

We investigated the impact of floxuridine, copper gluconate/TEA buffer, both copper gluconate/TEA buffer plus floxuridine, and copper-free buffer (10 mM sodium gluconate/180 mM TEA) on the solubility of irinotecan (all solutions adjusted to pH 7.0 pre- and post-addition of irinotecan). For these comparisons, sufficient irinotecan was added to provide a concentration of 85 mM if all drug was dissolved. This concentration was selected based on the calculated effective drug concentration inside CPX-1. In the absence of any added solutes, irinotecan, heated to 50°C and then allowed to cool to ambient temperature, provided a soluble concentration of 29 mM (Table IV). Addition of either floxuridine or copper gluconate/TEA individually to irinotecan (at concentrations present inside CPX-1 liposomes) resulted in an increase in irinotecan solubility to 46 and 48 mM, respectively. Interestingly, combining floxuridine and copper gluconate/TEA resulted in the highest level of irinotecan solubility at 62 mM (Table IV). This is in contrast to results obtained when irinotecan is exposed to the copper-free buffer where irinotecan solubility drops to 3 mM. It should be noted that upon solubilization of irinotecan at high concentrations in the presence of floxuridine plus copper gluconate/TEA, a well-defined flocculation characterized by rapid settling and a clear supernatant was formed.

Table IV. Solubility Assay for Irinotecan Demonstrates that CPX-1 Excipients Have a Notable Effect on Irinotecan Solubility

Buffer Condition	Irinotecan Concentration in solution (mM)
H_2O	29
90 mM floxuridine	46
100 mM copper gluconate/180 mM TEA	48
100 mM Copper gluconate/180 mM TEA+90 mM floxuridine	62
10 mM sodium gluconate/180 mM TEA	3

The theoretical maximum concentration of irinotecan is 85 mM based on the mass of drug weighed out and the volume of solvent. The concentration of floxuridine is 90 mM. See "MATERIALS AND METHODS" for a detailed description of buffer components.

Irinotecan Does Not Directly Interact with Copper Gluconate/TEA and Floxuridine

To further examine the influence of CPX-1 excipients on irinotecan solubility, isothermal titration calorimetry (ITC) and fluorescence studies were performed. Depending on the design and nature of the components involved, ITC can be used to quantitatively characterize the direct binding or partitioning of one substance into another (19). The heats generated by injecting 15 mM irinotecan into a solution of 5 mM floxuridine were of a magnitude on the order of the heats evolved from the heat of dilution upon injection of irinotecan into 100 mM HEPES at pH 7.0 (see Electronic supplementary material). The lack of any heats of interaction indicates that irinotecan does not directly interact with floxuridine.

Fluorescence emission scans were obtained for the titration of irinotecan in water in the presence of various excipients. The amount of fluorescence at 446 nm was plotted as a function of irinotecan concentration for aqueous solutions in the absence of added solutes or in the presence of floxuridine or copper gluconate/TEA (all at pH 7.0, see Electronic supplementary material). In all samples, fluorescence intensity increases similarly, up to an irinotecan concentration of approximately 200 μM after which successive quenching is observed with increasing irinotecan concentration. Peak intensity losses for 1 mM irinotecan in water, with 1 mM floxuridine or with 1 mM copper gluconate/TEA were calculated to be 42%, 36% and 34% respectively. The onset and degree of fluorescence quenching was comparable for all three irinotecan solutions.

Self-association of Irinotecan in Solution

Based on the calculated high intraliposomal concentration of irinotecan (85 mM) and its strong tendency for self-association (20), the majority of the intraliposomal drug would be expected to be oligomerized. UV–Vis spectroscopy was used here to verify this hypothesis. Monomeric irinotecan is characterized by two absorption peaks of near equal absorbance at approximately 358 and 370 nm (15,21,22). Upon dimerization/self-association, irinotecan exhibited a shifting and loss of absorbance from the higher wavelength peak (370 nm) in comparison to the lower wavelength peak (358 nm, see Electronic supplementary material). At concentrations of irinotecan in the millimolar range, its spectrum is characteristic of a dimer/oligomer as demonstrated by the sloping rather than biphasic shape of the spectra. By normalizing the spectra to the intensity at a single wavelength (358 nm), the change in shape becomes readily apparent (Fig. 4a). To examine spectral shifts at irinotecan concentrations which are relevant to defining the inner liposome environment of CPX-1, advantage was taken of a short pathlength quartz cuvette to gather data where irinotecan was in or near its dimer/aggregated state. The use of 1 mm pathlength cuvette allowed the self-association of irinotecan to be examined over relevant drug concentrations without signal saturation. By normalizing the spectra of Fig. 4a to a single wavelength, a binding association constant may be calculated. The two wavelengths selected with which to normalize the absorbance data were 358 and 365 nm. The total change in absorbance was determined from 10 to 1200 μM. The fractional change (θ) between these extremes was calculated and the data plotted as fractional change in absorbance *versus* total concentration of irinotecan ($[I]_{total}$; Fig. 4b). The equilibrium relationship was fit by the following derived partition function (Eq. 1):

$$\theta = \frac{K[I]_{\text{total}}}{(1 + K[I]_{\text{total}})} \tag{1}$$

where K represents the association constant.

Which can be used to determine dissociation constants (K_D) according to Eq. 2:

$$\theta = \frac{[I]_{\text{total}}}{(K_D + [I]_{\text{total}})} \tag{2}$$

The calculated dissociation constant was 260±50 μM so at loading conditions of 85 mM, there was approximately

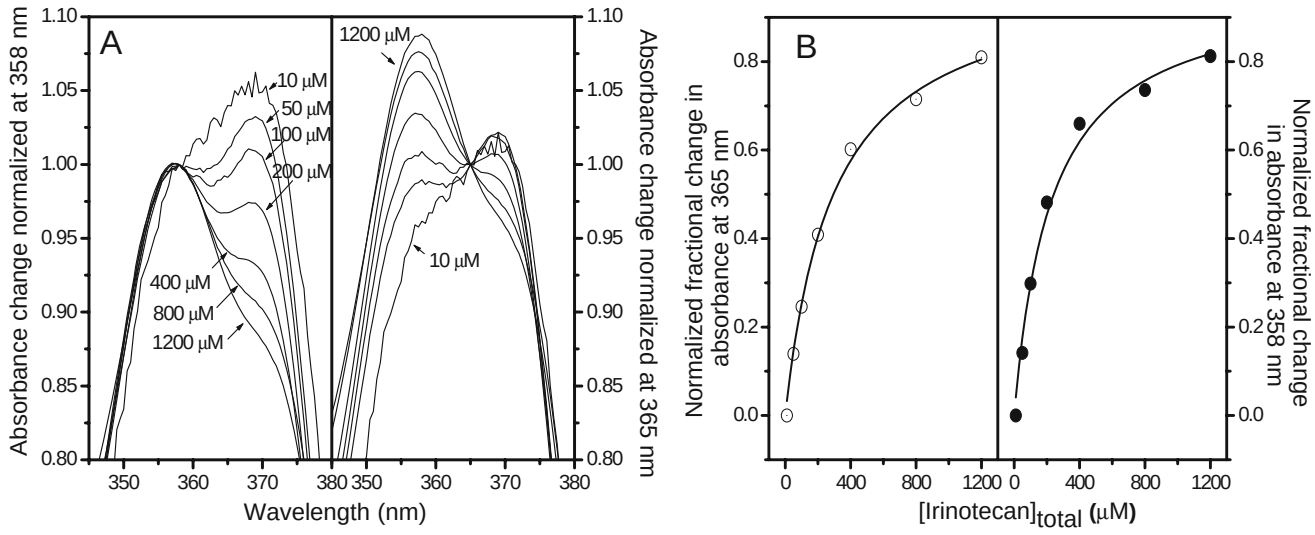

Fig. 4. **A** Change in absorbance of irinotecan, normalized at 358 nm (*left*) and 365 nm (*right*) for various concentrations. **B** Dissociation constant was generated by fitting the normalized change in absorbance *versus* total irinotecan concentration. Note that as it is not possible to generate an absorbance for 0 μM irinotecan, some error is introduced into the fit which is reflected in the line not passing through the 10 μM data point.

4.5 mM of monomeric irinotecan. This is consistent with irinotecan being predominantly in an oligomerized state in CPX-1. In addition, the spectral profile indicative of drug self-association was also observed at low pHs indicating that the aggregation of irinotecan was unaffected by its protonation state (data not shown).

DISCUSSION

CPX-1 is a liposomal formulation designed to maintain the synergistic 1:1 molar ratio of irinotecan and floxuridine in the plasma after i.v. administration while at the same time make the drugs bioavailable. In a previous study, we showed that the encapsulation of irinotecan was mediated by TEA in association with copper gluconate, leading to a final drug complex that is retained inside liposomes (15). However, the factors that controlled drug retention were not fully understood. The goal of the present study was to characterize the physical state of the drugs inside the liposomes and the potential interactions between drugs and excipients of CPX-1 in order to establish the parameters that dictate drug retention and ultimately the biological performance of this liposomal formulation. Also, in view of the potential clinical utility of drug combinations co-formulated in liposomal delivery systems, these investigations provide an approach to characterizing the biophysical properties of co-formulated drugs that can be applied to a range of different combinations.

The comparison of the *in vitro* release profile of the drugs in CPX-1 and copper-free formulations at comparable drug/lipid ratios revealed that the absence of copper gluconate had negligible effects on floxuridine release but was associated with decreased release of irinotecan. The lack of an observable change in either liposome morphology or internal structure by cryo-EM led to the hypothesis that the addition of copper gluconate might have some chemical and/or physical effect within the liposome that was manifested in augmented release characteristics for irinotecan in CPX-1. It should be noted that formation of copper-irinotecan and copper-topotecan complexes have been shown to result in drug precipitation inside liposomes that is observable by cryo-EM (14,23). We have previously reported that irinotecan was capable of forming a complex with unbuffered copper sulfate solution but unlikely with copper gluconate due to the presence of the strongly chelating gluconate ligands (log K= 18.2;15,24). The absence of a drug precipitate in CPX-1 is in line with the lack of direct copper gluconate–irinotecan interactions.

The biological activity of CPX-1 is dependent on the ability to reproducibly control drug retention within the liposomes such that the 1:1 molar ratio of irinotecan/floxuridine is maintained (2). Drummond *et al.* (13) and Ramsay *et al.* (23) have shown a correlation between increased drug retention and increased antitumor activity for irinotecan encapsulated liposomes. However, in the case of CPX-1, it is also necessary to coordinate the release of both drugs in order to prevent the formation of antagonistic ratios. In the case of irinotecan and floxuridine, the retention of the latter drug was first optimized by manipulating the lipid composition using low-cholesterol membranes (5). The irinotecan release was then manipulated to match the release of floxuridine. Consequently, this formulation represents conditions that maximize the retention of both drugs while avoiding the generation of antagonistic drug ratios which would arise if irinotecan retention was further increased. Thus, a thorough chemical and spectroscopic characterization of the states of irinotecan and floxuridine within CPX-1 and copper-free formulations was conducted in order to understand the basis for this controlled drug retention.

The most direct probe of the intraliposomal drugs' physical states was ^{1}H NMR. The aromatic protons of both irinotecan and floxuridine were easily detected and found to be sensitive to the presence of copper gluconate. In the case of floxuridine, this sensitivity was observed as paramagnetic line broadening; the two peaks at ~6.1 and ~7.8 ppm were relatively sharp and defined in the copper-free formulation but noticeably broadened in CPX-1 due to the presence of paramagnetic copper ions. Conversely, the four aromatic irinotecan molecules were more readily observed in CPX-1 compared to the copper-free formulation. Integration of peak intensities relative to an internal standard allowed for quantitation of observed floxuridine and irinotecan in both formulations (see Table II). For CPX-1, approximately 45% of the irinotecan could be observed; this value dropped to 19% in the copper-free formulation. Clearly, copper gluconate affects the physical state of irinotecan inside the liposomes. However, for the portion of irinotecan that could be observed in the CPX-1 and copper-free formulations, linewidth measurements suggest that the two species have similar properties.

Considering the known aggregation behaviour of irinotecan in solution (20), the NMR-silent portion of irinotecan is likely formed into a large aggregate that is rotationally immobile on the NMR timescale. Observation of protein ^{1}H resonances is limited by an upper limit on molecular weight of approximately 35–50 kDa (25). For globular proteins, molecules of this size have a spherical diameter of 5–7 nm, within the detection limit of cryo-EM given the defocus setting and ice thickness (0.5 μm) used in this work (16). Cryo-EM images of the copper-free and CPX-1 formulations, however, showed no evidence of large globular irinotecan aggregates, even in the copper-free formulation in which up to 81% of the available irinotecan would be presumed to be highly aggregated. Such observations would appear to be inconsistent with each other.

Predicted Morphology of Irinotecan Aggregates

Large molecular weight irinotecan aggregates are expected to form helical-like structures, based on the flat aromatic ring stacking of monomers with a slight twist of the overlapping aromatic planes predicted from UV–Vis, NMR and CD spectroscopy (20) and molecular modeling studies (data not shown). From simple computer imaging, irinotecan molecular dimensions are estimated as 22×7×2.5 Å with an intermolecular distance of 3.5 Å. Therefore, for an aggregate of N monomers, the aggregate length a is approximated by Eq. 3:

$$a = (2.5 \times N) + (3.5 \times (N - 1)) \quad (3)$$

The diameter is estimated as an average of the molecular planar axes lengths ((22+7)/2=14.5 Å) due to the helical twist between each monomer. Thus, the predicted shape of a large

irinotecan aggregate is most closely approximated by a prolate ellipsoid (Fig. 5).

Theoretical Prediction of Maximal Aggregate Size for NMR-Observed Irinotecan Fraction

Analysis of the linewidth of irinotecan proton resonances in the CPX-1 and copper-free formulations relative to the average proton linewidth of ubiquitin amide yields some insight into the size limit of NMR-observable irinotecan aggregates. Under conditions of constant temperature, the slow tumbling of macromolecules is the main determinant of the linewidth, due to the reduction in spin-spin relaxation time (T_2;18). For a spherical macromolecule, the rotational correlation time (τ_c) is related directly to molecular weight (M_r) from Stokes' Law (Eq. 4):

$$\tau_c = \frac{4\pi\eta_w r_H^3}{3k_B T} \quad (4)$$

$$\textit{where } r_H = \left(\frac{3\overline{V}M_r}{4\pi N_A}\right)^{\frac{1}{3}}$$

In the above equations, η_w is the solvent viscosity, k_B is the Boltzmann constant and T is temperature in Kelvin. The hydrodynamic radius (r_H) is estimated from the specific volume of the protein (typically 0.73 ml/g). Ubiquitin amide therefore has a calculated rotational correlation time of 3.8 ns for a hydrodynamic radius of 14 Å. Waters of hydration are neglected from the calculated radius.

Cavanagh *et al.* (17) used the relationships between spin-spin relaxation time (T_2) and rotational correlation time to construct a plot correlating the latter with observed linewidth. This relationship can be used to obtain an estimate of the rotational correlation time of an ubiquitin-like species that would have a proton resonant linewidth measured in the ^{1}H NMR spectrum of CPX-1. Given the observed NMR linewidths for irinotecan aggregates in the CPX-1 formulation of 29 and 56 Hz (Table III), correlation of these linewidths to Cavanagh's plot gives estimated observed rotational correlation times of 12 and 20 ns, respectively, for the NMR-observable portion of irinotecan in CPX-1.

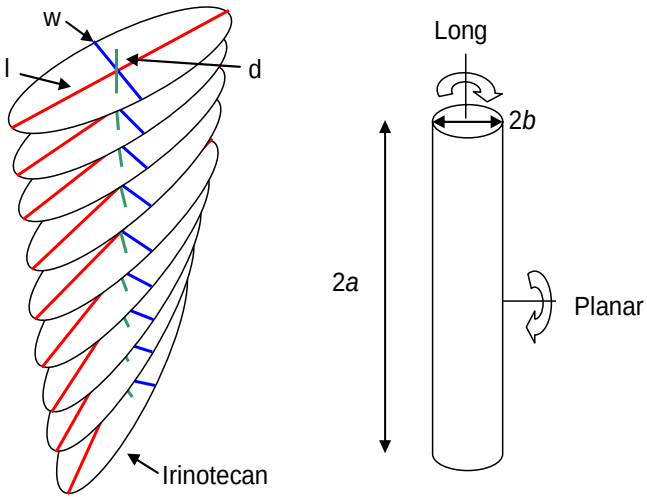

Fig. 5. *Left*: Schematic diagram of aggregated irinotecan showing individual molecular axes, length (l), width (w) and depth (d). *Right*: Rotation axes and semiaxes definition for a rod-like aggregate.

Rotational Diffusion of Ellipsoidal *Versus* Spherical Aggregates

The prediction above can be verified through calculation of rotational diffusion coefficients for both a spherical and ellipsoidal aggregate. Given the dimensions of the prolate ellipsoid with long and short axes a and b, Perrin reported the following equations for calculation of rotational diffusion coefficients of the major ($D_\parallel$, Eq. 5) and minor ($D_\perp$, Eq. 6) semiaxes of revolution (26–28):

$$D_\parallel = \frac{3k_B T}{32\pi\eta}\frac{2a - b^2 G(a,b)}{(a^2 - b^2)b^2} \quad (5)$$

$$D_\perp = \frac{3k_B T}{32\pi\eta}\frac{(2a^2 - b^2)G(a,b) - 2a}{a^4 - b^4} \quad (6)$$

where

$$G(a,b) = \frac{2}{(a^2 - b^2)^{\frac{1}{2}}}\ln\left(\frac{a + (a^2 - b^2)^{\frac{1}{2}}}{b}\right),$$

$$\textit{for } a > b \text{ (prolate ellipsoid)}$$

The rotational correlation times for an ellipsoid (three total) and sphere (isotropic, therefore one) are (29):

$$\tau_1 = (D_\parallel + 5D_\perp)^{-1} \quad (7a)$$

$$\tau_2 = (4D_\parallel + 2D_\perp)^{-1} \quad (7b)$$

$$\tau_3 = (6D_\perp)^{-1} \quad (7c)$$

$$\tau_{sphere} = (6D_o)^{-1} \quad (7d)$$

In NMR spectroscopy, for slow tumbling species, the observed linewidth would be generally dependent on the fastest rotational correlation time of the aggregate. For an ellipsoidal particle, it is expected that $D_\parallel > D_\perp$ due to the reduced displacement of solvent during rotation about the long axis. Therefore, τ_2 will yield the fastest rotational correlation time as it contains the largest contribution from $D_\parallel$. The rotational diffusion coefficients ($D_\parallel$, $D_\perp$) and τ_2 correlation times for ellipsoidal irinotecan aggregates of various sizes, along with spherical aggregates of an equivalent volume were calculated (see Electronic supplementary material). The highly impaired rotational diffusion about the planar axis is apparent in τ_3 which is solely dependent on $D_\perp$. For an aggregate of N=100, τ_3 is calculated to be 2.17 μs, compared to 15 ns for both τ_2 and a sphere of equivalent volume to the N=100 ellipsoid. This calculation demonstrates the dramatic loss in long axis mobility for a prolate ellipsoid relative to a sphere of the same volume. For N=100, the aggregate is estimated to be 60 nm long and 1.45 nm in

average diameter due to the helical twist of irinotecan aggregates. This rod-like ellipsoid has an identical volume as a sphere with a diameter of 5 nm. As stated above, a spherical aggregate of this size would be observable in the cryogenic electron micrograph presented herein. The ellipsoid shape, however, presents a small cross-sectional dimension across the long axis such that it is most accurately described as a filament and likely only visible by electron microscopy under the conditions used here, if packaged in a higher order assembly of the filaments. The cryo-EM images presented here do not give any indication of such behaviour.

The estimated rotational correlation times for liposomal irinotecan are 12–20 ns, depending on which observed linewidth is used (29 and 56 Hz, Table III). These times correlate to aggregates of 80–130 monomers, using the fastest rotational correlation time, τ_2 (see Electronic supplementary material). The aggregates would be expected to have dimensions of between 50 and 70 nm in length and identical diameters of 1.45 nm. This calculation gives an estimate on the NMR-observable irinotecan aggregate size and provides a mean by which irinotecan can form large macromolecular adducts yet remain undetected by conventional imaging methods. Presumably, the undetected irinotecan (55% in CPX-1 and 81% in the copper-free formulation) is aggregated such that the rotation is impaired and the augmented ^{1}H T_2 relaxation time is too fast for reliable NMR detection.

Intermolecular Limit to Aggregate Size for Observation of NMR Signals

An upper limit on the NMR-observable size is also predicted based on intermolecular interactions of discrete aggregate species. Above a certain number of polymer chains per unit volume, rod-like polymers or aggregates begin to influence the rotational tumbling of neighbouring chains, such

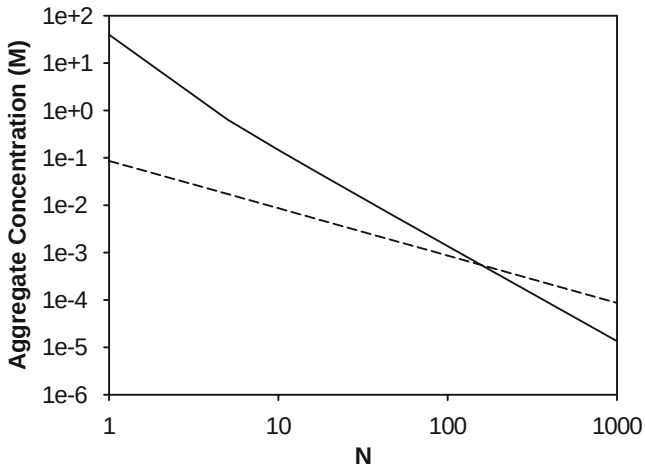

Fig. 6. Limit in rod-like aggregate concentration for isotropic rotational diffusion (*solid line*) as calculated from Eq. 8, with the actual irinotecan aggregate concentration for aggregates of size N (*dashed line*). Parameters used in the calculation were an encapsulated irinotecan concentration of 86 mM, and aggregate dimensions of $L = [(3.5\times N) + (2.5\times(N-1)]$ Å and d=14.5 Å. Aggregate concentration was calculated by dividing the total irinotecan concentration by N.

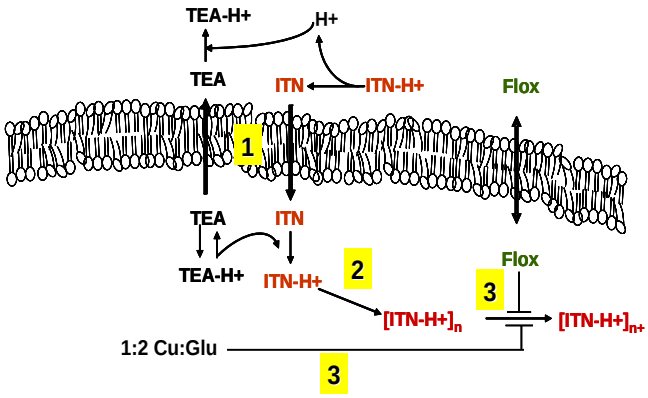

Fig. 7. Mechanism of drug loading of CPX-1, highlighting the neutral antiport active loading of irinotecan, the passive loading of floxuridine, and the roles of TEA and copper gluconate. *1* TEA is responsible for irinotecan loading via neutral antiport exchange mechanism. *2* Subsequent self-association of irinotecan enhances drug retention. *3* Copper gluconate/TEA and floxuridine together block large, higher order oligomerization of irinotecan via long-range interactions, thus allowing irinotecan to leak from the liposomes at the same rate as floxuridine.

that the rotational diffusion becomes anisotropic. This phenomenon is known as the log-jam effect for concentrated polymer solutions (30). Onsager (31) described the onset of this effect as a function of the rod dimensions in Eq. 8:

$$c_i = \frac{4.253}{dL^2} \tag{8}$$

Where d and L are the diameter and length of the polymer or aggregate rod, respectively, and c_i is the number of polymer units per unit volume. Division of the result by Avogadro's number yields the polymer concentration limit for isotropic tumbling behaviour. This calculation would assume a well behaved system of polymers/aggregates of narrow size distribution, with little to no flexibility in the rod.

For CPX-1, with an estimated internal irinotecan concentration of 85 mM, Eq. 8 can be used to calculate an upper limit on aggregate size (N) before the isotropic limit is exceeded and molecular tumbling is further impaired. Using the same aggregate dimensions as in the previous analysis, the change in the isotropic limit as a function of aggregate size can be calculated concurrently with the aggregate concentration. The latter is calculated simply as the total irinotecan concentration divided by the number of monomers per aggregate. These calculated values (isotropic limit from Eq. 8 and the actual irinotecan aggregate concentration) are plotted as a function of aggregate size N in Fig. 6. Examination of the intersection point of the calculated concentration with the isotropic limit gives an aggregate size of $N \leq 160$ monomers. This result suggests that for aggregates exceeding this size, isotropic rotation of the long rod-like aggregate will be steadily influenced by the presence of other neighbouring aggregate chains. Such interference will impair rotational diffusion, leading a reduction in T_2 relaxation time and loss of signal in the NMR experiment. This calculated result correlates and supports earlier calculations considering the slow axial tumbling of elongated prolate ellipsoids in solution.

Summary

The self-association of irinotecan in the presence of floxuridine and copper gluconate/TEA buffer was consistent with a long-range ordering and reduction of total charge in colloidal systems (32). At pH 7.0, the majority of irinotecan would be positively charged (pK_a=8.1), balanced by the partial negative charge of floxuridine (pK_a=7.4). This reduction in total charge modulates the aggregation of colloidal and positively-charged irinotecan by allowing for a closer approach of the suspended particles. Such long-range interactions are not typically detected by spectroscopic and calorimetric techniques, consistent with the ITC and fluorescence data presented here. Drugs–excipients interactions in CPX-1 serve to limit the size of irinotecan oligomers, greatly increasing the relative amount of irinotecan that exists in a rotationally mobile fraction that is NMR-detectable. The interplay between all excipients and drugs of CPX-1 is depicted in Fig. 7. The rate of irinotecan release is likely dependent on the oligomerization state of irinotecan inside the liposome, where larger, higher order oligomers are associated with decreased release rates. One role of copper gluconate in CPX-1 appears to be to inhibit large irinotecan aggregate formation. Taken together, the data presented here indicate that floxuridine and the excipients in CPX-1 maintain irinotecan in a physicochemical state that facilitates coordinated drug release and maintenance of the 1:1 molar drug ratio *in vivo*.

ACKNOWLEDGMENT

The authors would like to thank Dr. Sharon Johnstone for helpful discussions and Brianne O'Callaghan for technical support. We would like to recognize the superior NMR service provided by Drs. Maria Ezhova and Nick Burlinson at the University of British Columbia NMR Facility. We are also grateful to Goran Karlsson and Dr. Katarina Edwards at Uppsala University in Sweden for the cryo-EM work.

REFERENCES

1. S. Sengupta, D. Eavarone, I. Capila, G. Zhao, N. Watson, T. Kiziltepe, and R. Sasisekharan. Temporal targeting of tumor cells and neavasculature with a nanoscale delivery system. *Nature*. **436**:568–572 (2005).
2. L. D. Mayer, T. O. Harasym, P. G. Tardi, N. L. Harasym, C. R. Shew, S. A. Johnstone, E. C. Ramsay, M. B. Bally, and A. S. Janoff. Ratiometric dosing of anticancer drug combinations: controlling drug ratios after systemic administration dictates therapeutic activity in tumor-bearing mice. *Mol. Cancer. Ther.* **5**:1854–1863 (2006).
3. T. O. Harasym, P. G. Tardi, S. A. Johnstone, L. D. Mayer, M. B. Bally, and A. S. Janoff. Fixed drug ratio liposomes formulations of combination cancer therapeutics. In G. Gregoriadis (ed.), *Liposome Technology, 3rd ed.*, CRC, Boca Raton, FL, 2007, pp. 25–48.
4. X. Zhao, J. Wu, N. Muthusamy, J. C. Byrd, and R. J. Lee. Liposomal coencapsulated fludarabine and mitoxantrone for lymphoproliferative disorder treatment. *J. Pharm. Sci.* **97**:1508–1572 (2007).
5. P. G. Tardi, R. C. Gallagher, S. A. Johnstone, N. Harasym, M. Webb, M. B. Bally, and L. D. Mayer. Co-encapsulation of irinotecan and floxuridine into low cholesterol-containing liposomes that coordinate drug release *in vivo*. *Biochim. Biophys. Acta*. **1768**:678–687 (2007).
6. G. Batist, K. Chi, W. Miller, S. Chia, F. Hasanbasic, A. Fisic, L. M. Mayer, C. Swenson, A. S. Janoff, and K. Gelmon. Phase I study of CPX-1, a fixed ratio formulation of irinotecan (iri) and floxuridine (flox), in patients with advanced solid tumors. ASCO Annual Meeting. 2014 (2006).
7. G. Batist, W. Miller, L. Mayer, A. Janoff, C. Swenson, A. Louie, K. Chi, S. Chia, and K. Gelmon. Ratiometric dosing of irinotecan (IRI) and floxuridine (FLOX) in a phase I trial: A new approach for enhancing the activity of combination chemotherapy. *J. Clin. Oncol*. **25**:109s (2007).
8. T. O. Harasym, P. G. Tardi, N. L. Harasym, P. Harvie, S. Johnstone, and L. D. Mayer. Increased preclinical efficacy of irinotecan and floxuridine co-encapsulated inside liposomes is associated with tumor delivery of synergistic drug ratios. *Oncol. Res.* **16**:361–374 (2007).
9. L. D. Mayer, and A. S. Janoff. Optimizing combination chemotherapy by controlling drug ratios. *Mol. Interv*. **7**:216–223 (2007).
10. Y. Barenholz, S. Amselem, D. Goren, R. Cohen, D. Gelvan, A. Samuni, E. B. Golden, and A. Gabizon. Stability of liposomal doxorubicin formulations: problems and prospects. *Med. Res. Rev*. **13**:449–491 (1993).
11. M. Grit, and D. J. Crommelin. Chemical stability of liposomes: Implications for their physical stability. *Chem. Phys. Lipids*. **64**:3–18 (1993).
12. C. O. Noble, M. T. Krauze, D. C. Drummond, Y. Yamashita, R. Saito, M. S. Berger, D. B. Kirpotin, K. S. Bankiewicz, and J. W. Park. Novel nanoliposomal CPT-11 infused by convection-enhanced delivery in intracranial tumors: pharmacology and efficacy. *Cancer Res*. **66**:2801–2806 (2006).
13. D. C. Drummond, C. O. Noble, Z. Guo, K. Hong, J. W. Park, and D. B. Kirpotin. Development of a highly active nanoliposomal irinotecan using a novel intraliposomal stabilization strategy. *Cancer Res*. **66**:2171–2177 (2006).
14. A. S. Taggar, J. Alnajim, M. Anantha, A. Thomas, M. Webb, E. Ramsey, and M. B. Bally. Copper-topotecan complexation mediates drug accumulation into liposomes. *J. Control. Release*. **114**:78–88 (2006).
15. A. Dicko, P. G. Tardi, X. Xie, and L. D. Mayer. Role of copper gluconate/triethanolamine in irinotecan encapsulation inside the liposomes. *Int. J. Pharm*. **337**:219–228 (2007).
16. M. Almgren, K. Edwards, and G. Karlsson. Cryo transmission electron microscopy of liposomes and related structures. *Colloids Surf. A*. **174**:3–21 (2000).
17. J. Cavanagh, A. G. Palmer III, W. J. Fairbrother, N. J. Skelton, and M. Rance. *Protein NMR Spectroscopy: Principles and Practice*. Academic, San Diego, 1996.
18. G. S. Rule, and T. K. Hitchens. *Fundamentals of Protein NMR Spectroscopy*. Springer, Berlin, 2005.
19. T. Wiseman, S. Williston, J. F. Brandts, and L. N. Lin. Rapid measurement of binding constants and heats of binding using a new titration calorimeter. *Anal. Biochem*. **179**:131–137 (1989).
20. R. Aiyama, H. Nagai, S. Sawasa, T. Yokokura, H. Itokawa, and M. Nakanishi. Determination of self-association of irinotecan hydrochloride (CPT-11) in aqueous solution. *Chem. Pharm. Bull*. **40**:2810–2813 (1992).
21. I. Chourpa, J.-M. Millot, G. D. Sockalingum, J.-F. Riou, and M. Manfait. Kinetics of lactone hydrolysis in antitumor drugs of camptothecin series as studied by fluorescence spectroscopy. *Biochim. Biophys. Acta*. **1379**:353–366 (1998).
22. I. Nabiev, F. Fleury, I. Kudelina, Y. Pommier, F. Charton, J.-F. Riou, A. J. Alix, and M. Manfait. Spectroscopic and biochemical characterization of self-aggregates formed by antitumor drugs of the camptothecin family. *Biochem. Pharmacol*. **55**:1163–1174 (1998).
23. E. Ramsay, J. Alnajim, M. Anantha, J. Zastre, H. Yan, M. Webb, D. Waterhouse, and M. Bally. A novel liposomal irinotecan formulation with significant anti-tumor activity: Use of the divalent cation ionophore A23187 and copper-containing liposomes to improve drug retention. *Eur. J. Pharm. Biopharm.* (2008) in press.
24. L. Pecsok, and R. S. Juvet Jr. The gluconate complexes. I. Copper gluconate in strongly basic media. *J. Am. Chem. Soc.* **77**:202–206 (1955).

25. H. Yu. Extending the size limit of protein nuclear magnetic resonance. *Proc. Natl. Acad. Sci. U. S. A*. **96**:332–334 (1999).
26. F. Perrin. The Brownien [sic] movement of an ellipsoide [sic]—The dielectric dispersion of ellipsoidal molecules. *J. de Phys. et Rad.* **5**:497–511 (1934).
27. F. Perrin. Brownian movement of an ellipsoid (ii): free rotation and fluorescence depolarization. Translation and diffusion of ellipsoidal molecules. *J. de Phys. et Rad.* **7**:1–11 (1936).
28. G. A. Barrall, K. Schmidt-Rohr, Y. K. Lee, K. Landfester, H. Zimmermann, G. C. Chingas, and A. Pines. Rotational diffusion measurements of suspended colloidal particles using two-dimensional exchange nuclear magnetic resonance. *J. Chem. Phys*. **104**:509–520 (1996).
29. J. R. Lakowicz. Principles of Fluorescence Spectroscopy (3rd ed.). Springer Science + Business Media, Singapore, 2006.
30. E. C. Chung, and J. Chung. Rotational diffusion coefficient of rod-like polymer with a slight flexibility in semidilute and concentrated solutions. *Poly. Bull*. **21**:105–112 (1989).
31. L. Onsager. The effects of shape on the interaction of colloidal particles. *Ann. N.Y. Acad. Sci*. **51**:627–659 (1949).
32. A. R. Gennaro (Ed.). Remington: The Science and Practice of Pharmacy, 20th ed., Lippincott Williams & Wilkins, Philadelphia, 2000.